Revista Brasileira de Agricultura Irrigada
Brazilian Journal of Irrigated Agriculture
ISSN: 1982-7679 (on-line)
v.18, p. 96 - 108, 2024
Fortaleza, CE - www.inovagri.org.br

DOI: 10.7127/rbai.v1801350

WATER DISTRIBUTION CHARACTERISTICS OF DEFLECTOR PLATES USED IN CENTER PIVOT IRRIGATION SYSTEMS

CARACTERÍSTICAS DE DISTRIBUIÇÃO DE ÁGUA DE PLACAS DEFLETORAS EMPREGADAS EM PIVÔS CENTRAIS

Giuliani do Prado[1], Tiago Bueno Braga Coelho[2] Adriano Catossi Tinos[3] , Edmilson Cesar Bortoletto[4] , Denise Mahl[5], Daniela D'Orazio Bortoluzzi[5]

[1]Professor, Departamento de Engenharia Agrícola (DEA), Universidade Estadual de Maringá – UEM, Paraná, Brasil
[2]Aluno do curso de Engenharia Agrícola da Universidade Estadual de Maringá – UEM, Paraná, Brasil
[3] Engenheiro Agrícola, Departamento de Engenharia Agrícola (DEA), Universidade Estadual de Maringá – UEM, Paraná, Brasil
[4] Professor, Departamento de Engenharia Agrícola (DEA), Universidade Estadual de Maringá – UEM, Paraná, Brasil
[5]P Professora, Departamento de Engenharia Agrícola (DEA), Universidade Estadual de Maringá – UEM, Paraná, Brasil

ABSTRACT: The work aimed to determine the water distribution characteristics of the spray-sprinkler Asfix type manufactured by Fabrimar®. In the evaluations, 96 combinations were considered, given by: working pressure (103 and 138 kPa), sprinkler height (0.8, 1.6, and 2.4 m), nozzle diameter (4.4 and 5.6 mm), and deflector plates (two rotating and six fixed). The water application rates were measured from radial rows of collectors. The mean application rate values were used to determine the wetted radii and the water distribution curves. The distribution curves were normalized and processed with the cluster analysis employing the K-Means method. Power equations of wetted radius, as a function of nozzle diameter, working pressure, and sprinkler height, presented coefficients of determination higher than 90%. Four representative shapes of distribution curves for deflector plates yellow, red, blue, and purple, as well as white, black, gray, and green, resulted, respectively, in standard deviations of 0.191 and 0.219. Sprinkler working with fixed plates had a trend to present high application rates near the edge of the water distribution curve. However, rotating plates (yellow and red) provided a decrease in application rate along the distribution curve.

Keywords: rotating plate, fixed plate, distribution curve.

RESUMO: O trabalho objetivou determinar as características de distribuição de água do aspersor Asfix produzido pela Fabrimar®. Nas avaliações foram consideradas 96 condições dadas por: pressão de serviço (103 e 138 kPa), altura de instalação (0,8, 1,6 e 2,4 m), diâmetro do bocal (4,4 e 5,6 mm) e placas defletoras (duas rotativas e seis fixas). As intensidades de aplicação de água foram mensuradas a partir de linhas radiais de coletores. Os valores médios de intensidade de aplicação foram empregados na determinação dos raios de alcance e dos perfis radiais de aplicação de água. Os perfis radiais foram adimensionalizados e submetidos a análise de agrupamento pelo método K-Means. Equações potenciais de raio de alcance, em função do diâmetro do bocal, pressão de serviço e altura do aspersor apresentaram coeficientes de determinação superiores a 90%. Tanto para as placas amarela, vermelha, azul e roxa, como para as branca, preta, cinza e verde, quatro perfis representativos resultaram, respectivamente, em desvios médios de 0,191 e 0,219. Condições operacionais associadas às placas defletoras fixas tenderam a apresentar um acúmulo de água na extremidade final do perfil radial. Todavia, as placas defletoras rotativas (amarela e vermelha) proporcionaram um decréscimo na intensidade de aplicação de água ao longo do perfil radial.

Palavras-chave: placa rotativa, placa fixa, perfil radial.

Protocolo 1350.27-03-2023- Aprovado em 23-10-2024
* Autor correspondente: gprado@uem.br
Editor de área: Ana Nascimento

INTRODUCTION

The food demand due to population growth should be supplied via increasing cultivated areas and improving crop techniques (WANG et al., 2022; CHARFI et al., 2021). In this context, irrigation has been a vital tool for raising the quantity and quality of crop production. According to the Brazilian capacity of infrastructure, soil, and topography, the country could expand its irrigated areas by 55.85 million hectares (ANA, 2021).

By virtue of automation, irrigation of large areas, and suitable efficiency and uniformity values, center pivot systems have been widely employed (AL-GHOBARI; DEWIDAR, 2021). Over the improvement of this irrigation system, high-pressure impact sprinklers have been replaced by spray-type sprinklers that operate at low pressure, which can reduce the amount of energy consumption (HUI et al., 2021).

These low-pressure sprinklers have deflector plates, which can be fixed or rotating (VALENCIA et al., 2019). In accordance with the authors, rotating-plate sprinklers have presented better water distribution than fixed-plate sprinklers, but the latter has a lower cost to purchase. Nevertheless, proper selection of working combinations can result in similar water application uniformity regardless of plate type. The ideal working arrangement for irrigation systems to reach high uniformity can be set during the project design based on digital simulations. Therefore, the technical data of water distribution from the sprinklers (water distribution curve) working under distinct operations have been essential (ZHANG et al., 2019).

Rovelo et al. (2019) pointed out that few technical data on account of water distribution curves have been published by sprinkler manufacturers. Thus, this work aimed to determine representative geometric shapes of the water distribution curve from a sprinkler working under different configurations of working pressure, nozzle diameter, type of deflector plate, and sprinkler height.

MATERIAL AND METHODS

The work was carried out at Universidade Estadual de Maringá (UEM), Campus do Arenito (CAR), in Cidade Gaúcha county, Paraná state, to evaluate the water distribution patterns of the sprinkler Asfix manufactured by Fabrimar®. This spray sprinkler is composed of a single nozzle and a deflector plate, and it has been recommended to center pivot and lateral move irrigation systems. The water distribution patterns were determined for 96 working combinations, given by: a) two working pressures (103 and 138 kPa); b) two nozzle diameters (4.4 and 5.6 mm); c) three sprinkler mounting heights from the water collectors (0.8, 1.6, and 2.4 m), and; d) eight deflector plates (Figure 1).

Red rotating plate: angle of 12º		Yellow rotating plate: angle 21º	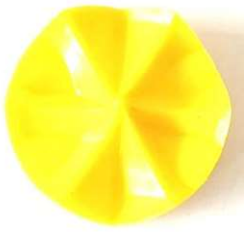
Blue fixed plate: concave shape with 36 grooves		Purple fixed plate: flat shape and smooth	
White fixed plate: convex shape with 36 grooves		Black fixed plate: flat shape with 34 fine grooves	
Gray fixed plate: triangular shape with 32 thick grooves		Green fixed plate: flat shape with 24 thick grooves	

Figure 1. Sprinkler deflector plates employed in the water distribution tests.

In order to measure the water distribution patterns under no-wind conditions, a test bench was set up near the Laboratory of Hydraulics and Irrigation at UEM/CAR. The apparatuses employed to assemble this test bench were set by: i) a water reservoir; ii) a centrifugal pump; iii) a line of pipes with gate valves, a disc filter, and a water flow meter; iv) a digital pressure gauge (scale from 0 to 5 kgf cm-2), and; v) radial rows of water collectors. Due to the symmetrical shape of water applied onto the sprinkler-wetted circle in no-wind conditions (LIU, et al., 2018), only a quadrant of the wetted circle was considered to measure the water sprinkled. Hence, water collectors of eight centimeters in diameter and 0.5 m apart from each other were located along seven radial rows (Figure 2).

Assuming the quadrant (0 to 90º) origin at zero degrees, the rows 1 (L1) and 7 (L7) were put down, respectively, at 2.5 and 87.5º and, the others (L2, L3, L4, L5, and L6) were set apart at an angular distance of 14º10'.

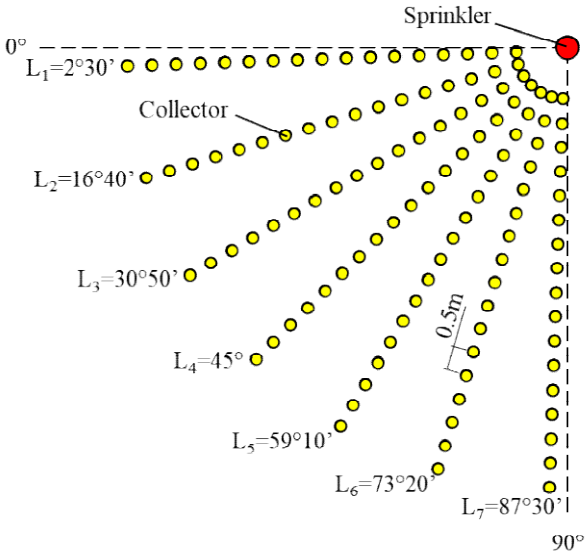

Figure 2. Layout of water collector rows on the test bench to catch the water applied by the sprinkler.

Each test duration was one hour long, and within this period, the working pressure was monitored with the digital pressure gauge situated in the same plane as the sprinkler nozzle.

The amount of water applied (volume) was measured on the flow meter, and forty minutes long was considered to determine the sprinkler flow rate. After the test, the volume of water caught in every collector was quantified using a graduated cylinder with a capacity of 100 cm3. The average volume value observed in collectors at the same radial distance from the sprinkler was divided by the transverse collector area and converted into application rate.

The application rate data determined to set the mean water distribution curve was used to compute the sprinkler wetter radius, which represents the furthest distance to the sprinkler where was observed a rate of 0.25 mmh-1, according to ISO 8026 (ISO, 2009). In the process of calculating the mean water distribution curve, collector rows 1 and 4 (Figure 2) were discarded, respectively, due to splashes caused by a concrete pillar and the influence of the sprinkler rod.

The values of flow rate and sprinkler wetted radius under different working combinations were adjusted by the least squares method, respectively, to Equations 1 and 2.

$$q = a_1 * n^{a2} * p^{a3} \quad (1)$$

$$R = a_4 * h^{a5} * n^{a6} * p^{a7} \quad (2)$$

Where: q - sprinkler flow rate (m3 h-1); R - sprinkler wetted radius (m); n - nozzle diameter (mm); p - working pressure (kPa); h - sprinkler height (m), and; a1, a2, a3, a4, a5, a6 and a7 - fitting coefficients of the equations.

Considering combinations of working pressure (p) and nozzle diameter (n), decreasing in the wetted radius with the sprinkler mounting height to the wetted radius determined by the sprinkler height at 2.4 m was computed by:

$$D_R = \frac{(R_h - R_{2.4})}{R_{2.4}} * 100 = \left[\left(\frac{h}{2.4}\right)^{a5} - 1\right] * 100 \quad (3)$$

Where: DR - decreasing in the sprinkler wetted radius (%); Rh - wetted radius for the sprinkler mounting height h (m), and; R2,4 - wetted radius for the sprinkler mounting height at 2.4 m. Aiming to avoid volumetric errors in digital simulations (PRADO, 2016), at the

end of each water distribution test, the mean application rate values, as a function of radial distance to the sprinkler, were used to estimate the flow rate applied by the sprinkler:

$$q_p = \frac{2*\pi}{1000} * \int_0^R i(r)*r*dr \quad (4)$$

Where: qp - flow rate estimated from the water distribution curve (m3 h-1); i(r) - application rate as function of radial distance to the sprinkler (mm h-1), and; r - radial distance of a water collector to the sprinkler (m). According to Solomon and Bezdek (1980) methodology, the water distribution curves were normalized. Thus, the radial distances to the sprinkler were set as a fraction of the wetted radius (Equation 5) and the application rate values as a fraction of the average water application rate (Equation 6).

$$r_d = \frac{r}{R} \quad (5)$$

$$i_d = \frac{i_c * \pi * R^2}{1000 * q_p} \quad (6)$$

Where: rd - dimensionless radial distance to the sprinkler (-), and; id - dimensionless water application rate (-).

The dimensionless water distribution curves were submitted to clustering analysis using the K-Means method described by Solomon and Bezdek (1980). Two clustering analysis were processed, one employing the dimensionless water distribution curves set to deflector plates yellow, red, blue, and purple (48 curves) and another to deflector plates white, black, gray, and green (48 curves).

In order to run the clustering analysis, twenty application rates were set for every dimensionless water distribution curve using the cubic spline interpolation algorithm (BURDENS; FAIRES, 2003). The dimensionless radial distances to the sprinkler were given by Equation 7.

$$r_d = 0.025 + (j-1)*0.05 \quad (7)$$

Where: j - radial distance index from 1 to 20.

RESULTS AND DISCUSSION

Average values of flow rate, coefficient of variation, and flow rate given in the manufacture technical catalog as a function of nozzle diameter and sprinkler working pressure are presented in Table 1. The accuracy of the flow rate measurements in the tests can be denoted by the coefficients of variation lower than 1% and the average difference of 1.98% between flows measured and provided by the manufacturer. ISO standard 8026 (ISO, 2009) quotes the average flow rate shall not deviate by more than 2.5% from the nominal flow rate.

Table 1. Average flow rate (qa), coefficient of variation (CV), and flow rate informed by the manufacturer (qm) as function of nozzle diameters (n) and working pressures (p).

n (mm)	p (kPa)	q_a (m^3 h^{-1})	CV (%)	q_m (m^3 h^{-1})
4.4	103	0.769	0.812	0.750
	138	0.886	0.867	0.850
5.6	103	1.200	0.974	1.210
	138	1.375	0.951	1.370

The ninety-six flow rate data set in the tests were employed to fit a power equation with nozzle diameter and working pressure as independent variables (Figure 3). According to the coefficient of determination obtained, the flow rate outcomes computed by this equation can be explained at 99.83%.

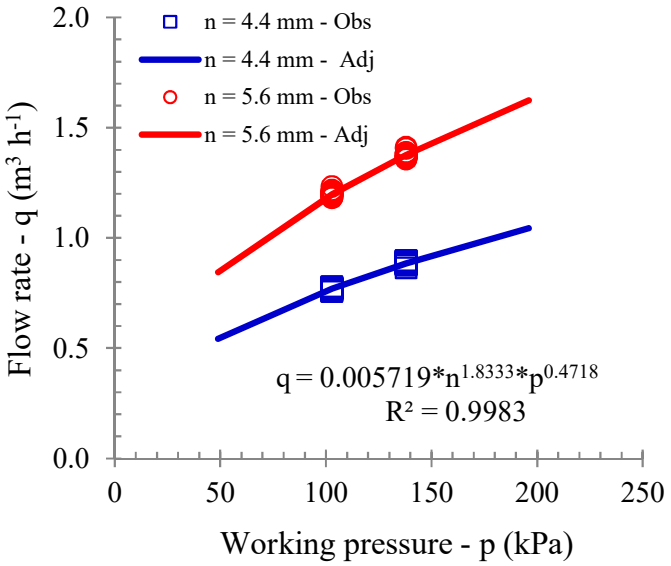

Figure 3. Observed (Obs) and adjusted (Adj) flow rate (q) data as a function of working pressure (p) to the sprinkler with nozzle diameter (n) of 4.4 and 5.6 mm.

.

Prado et al. (2021) used flow rate data measured for 144 combinations of nozzle diameters and working pressures to fit a power equation, and a coefficient of determination (R2 = 0.9996) near one was observed. The authors mentioned that a power equation as a function of nozzle diameter and working pressure has been suitable for modeling the flow rate data. Furthermore, a pressure head exponent equal to 0.5 (LIU et al., 2018), or close to it, has been commonly found for these equations. Regarding the same deflector plate, combinations of nozzle diameter, working pressure, and sprinkler mounting height resulted in a range of wetted radii (Table 2). Rotating plates (yellow and red) reached larger wetted radii than the fixed plates, and the flat fixed plate (purple) presented the lowest average value. Evaluating fixed and rotating plate sprinklers under a pressure of 103 kPa, a sprinkler mounting height of 0.8 m, and three nozzle diameters (2.78, 4.76, and 6.75 mm), Jiao et al. (2017) verified wetted radii values that, respectively, ranged from 5.02 to 6.85 m and 4.88 to 7.05 m.

Table 2. Range of wetted radius measured in the tests for each deflector plate, maximum (Rmax), average (Rave), and minimal values (Rmin).

Deflector Plate	R_{max} (m)	R_{ave} (m)	R_{min} (m)
Yellow	7.846	6.954	6.056
Red	8.150	7.068	6.000
Blue	6.742	5.626	4.583
Purple	5.200	4.403	3.522
White	5.750	4.524	3.013
Black	7.391	5.502	4.004
Gray	7.400	5.911	4.532
Green	7.478	5.521	3.554

Based on the wetted radii measured, as a function of sprinkler height, working pressure, and nozzle diameter, power equations were fitted for each deflector plate type, and coefficients of determination higher than 90% were found (Table 3). Concerning the same independent variables, Sayyadi et al. (2014) set wetted radius equations for sprinklers working with fixed deflector plates and observed in the regression analysis coefficients of determination from 93 to 96%.

Table 3. Wetted radius (R in m) equations and coefficients of determination (R2) for the deflector plates as a function of nozzle diameter (n in mm), sprinkler height (h in m), and working pressure (p in kPa).

Deflector plate	Equation	R^2
Yellow	$R=2.8181*h^{0.1865}*n^{0.1530}*p^{0.1222}$	0.9779
Red	$R=2.0401*h^{0.1834}*n^{0.1191}*p^{0.2048}$	0.9496
Blue	$R=0.3828*h^{0.1879}*n^{0.3492}*p^{0.4291}$	0.9050
Purple	$R=1.5509*h^{0.2684}*n^{0.2035}*p^{0.1274}$	0.9499
White	$R=0.4722*h^{0.3654}*n^{0.4251}*p^{0.2984}$	0.9594
Black	$R=0.5015*h^{0.3937}*n^{0.6281}*p^{0.2557}$	0.9713
Gray	$R=0.8036*h^{0.3023}*n^{0.3888}*p^{0.2611}$	0.9690
Green	$R=0.2604*h^{0.4106}*n^{0.4121}*p^{0.4643}$	0.9628

Changing the sprinkler mounting height by one meter, an average variation of 1.07 m in the wetted radius was found. In relation to the sprinkler mounting height of 2.4 m, the percentage values of the wetted radius decrease are depicted in Figure 4. Bringing down the sprinkler mounting height from 2.4 to 0.8 m, a reduction of -18.5, -18.3, and -18.7% on the wetted radius was computed, respectively, to sprinkler plates yellow, red, and blue. On the other hand, the

sprinkler with deflector plates purple and grey presented, respectively, decreases of -25.5 and -28.3% on the wetted radius, and the deflector plates white (-33.1%), black (-35.1%), and green (-36.3%) had the largest diminutions..

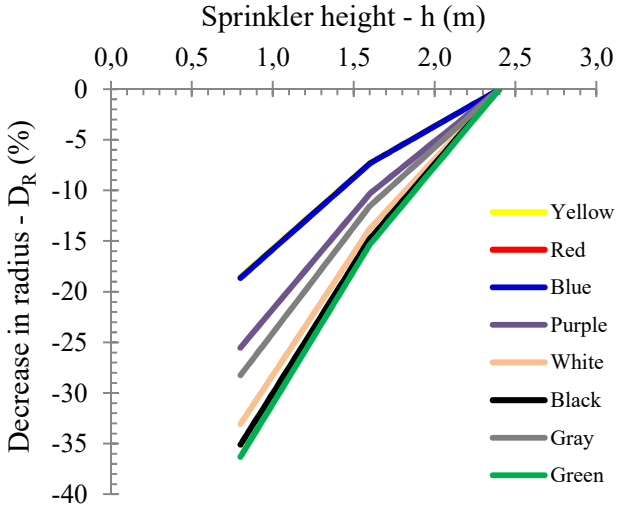

Figure 4. Decrease in the distance of wetted radius for each deflector plate as a function of the sprinkler mounting height.

In the evaluation of a sprinkler with a fixed deflector plate (36 grooves) under combinations of nozzle diameter (4.76 mm), working pressures (50, 100, 150, and 200 kPa), and sprinkler mounting heights (0.5, 1.0, 1.5, 2.0, and 2.5 m), Zhang et al. (2019) had a mean variation of 0.72 m in the wetted radius by altering the sprinkler mounting height in one meter. In addition, a reduction in the sprinkler mounting height from 2.5 to 0.5 m resulted in an average decrease of -39.8% in the wetted radius. Due to similarities in the dimensionless water distribution curves observed, it was processed two clustering analysis by the K-Means method (Figure 5). Hence, the dimensionless water curves determined from deflector plates yellow, red, blue, and purple (48 curves) were employed in the first clustering analysis (Figure 5A), and the normalized curves set from deflector plates white, black, gray, and green (48 curves) were processed in a second clustering analysis (Figure 5B).

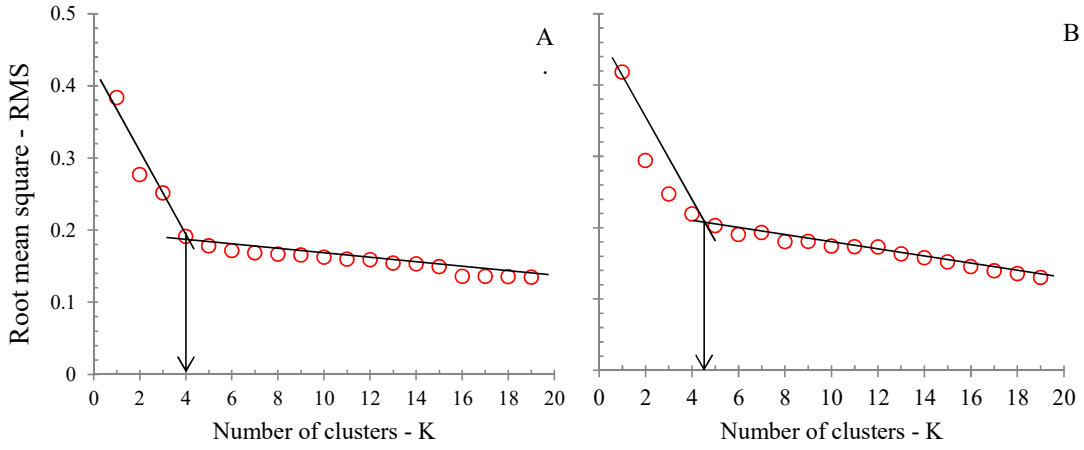

Figure 5. Standard deviation due to K-number of water distribution shapes processed in K-Means analysis for deflector plates yellow, red, blue, and purple (A) and gray, black, white, and green (B).

According to Solomon and Bezdek (1980), the most appropriate number of shapes to represent the water distribution curves can be set around the region of a sharp change in slopes of standard deviation (RMS) as a function of the K-number of clusters. Therefore, the two clustering analyses revealed that four water distribution shapes (K = 4) resulted in standard deviations (RMS) of 0.191 and 0.219, respectively, to the first (Figure 5A) and second (Figure 5B) data sets processed by the K-Mean algorithm.

The geometrical shapes, which represent the dimensionless water distribution curves from the first (yellow, red, blue, and purple plates) and second (white, gray, black, and green plates) clustering analysis, are depicted in Figures 6 and 7. In these figures, the vertical bars on the shape curves indicate one standard deviation of the dimensionless water application rate value.

An evident decrease in the water application rate along the distance from the sprinkler on the water distribution shapes I and II has been presented in Figure 6. However, the water distribution patterns III and IV (Figure 6) provided high application rates, respectively, at intervals of relative distances from 0.2 to 0.8 and 0.2 to 0.5. Comparing these water distribution shapes with the geometrical patterns defined by Christiansen (1942) to sprinklers, it can be assumed that geometric shapes I, II, and III resemble Christiansen's theoretical patterns C, A, and E. The water distribution curve IV has no similarity to the water distribution patterns described by Christiansen (1942).

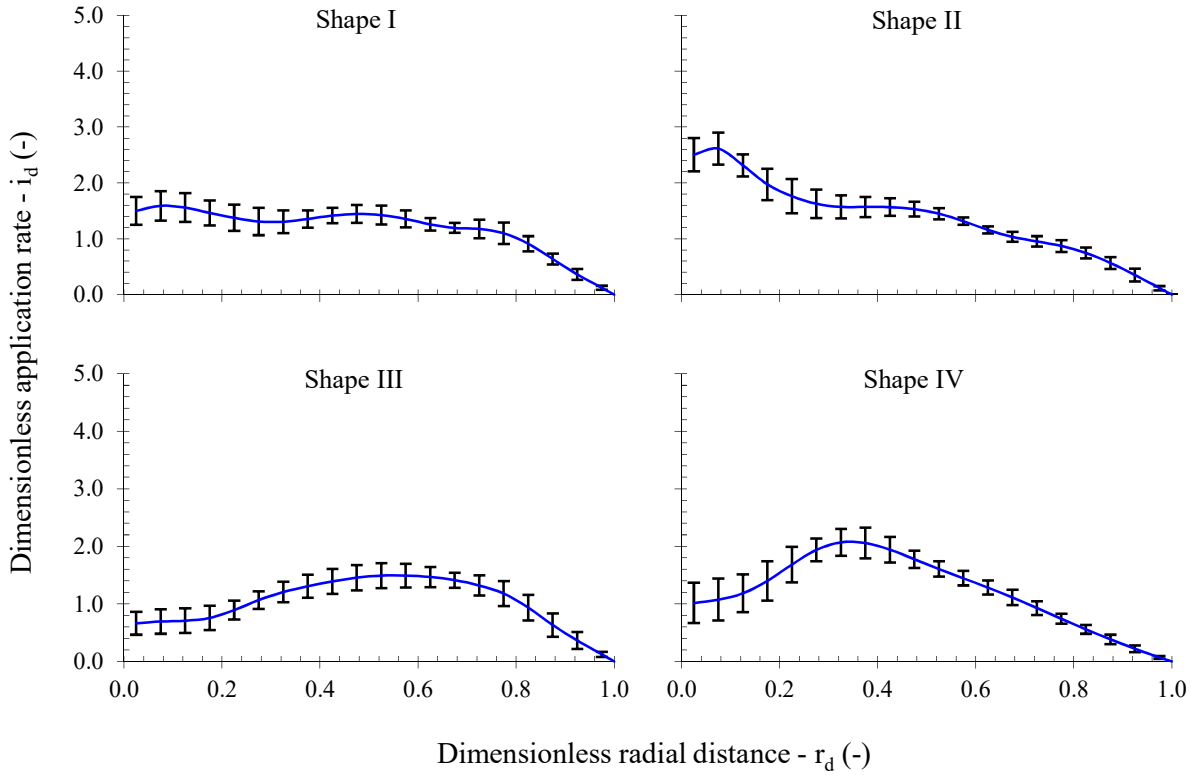

Figure 6. Dimensionless shapes of water distribution curves from the sprinkler working with deflector plates: yellow, red, blue, and purple

The prototypical dimensionless water distribution curves from the white, black, gray, and green deflector plates (Figure 7) had low water application rate values (less than 1) over the relative distance between 0 to 0.6 and, from this point on, the values had sharp increases, which reaches dimensionless application rate values up to 3 near the wetted circle edge.

According to Rovelo et al. (2019), rotating spray plate sprinklers provide water distribution curves with triangular shapes, and fixed spray plate sprinklers with doughnut or ring shapes.

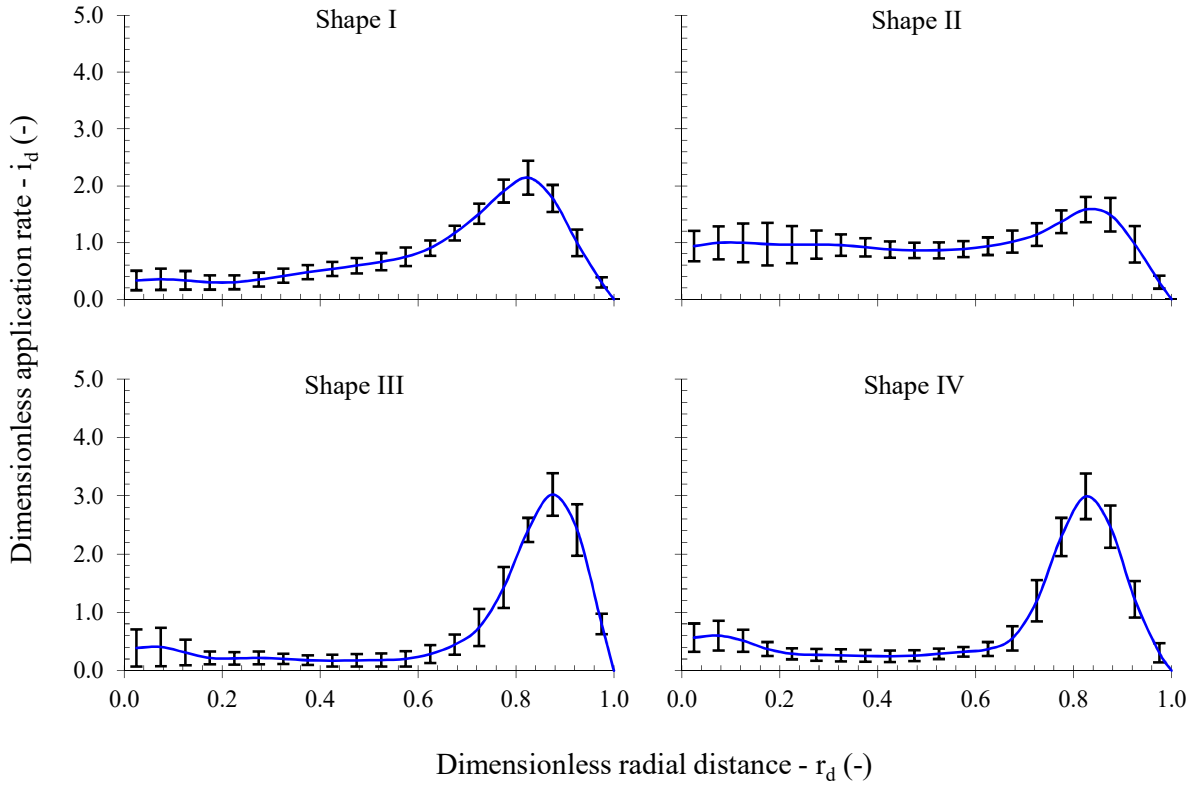

Figure 7. Dimensionless shapes of water distribution curves from the sprinkler working with deflector plates: white, black, gray, and green.

Combinations of nozzle diameter, working pressure, and sprinkler height, which define a representative geometric shape of the water distribution curves, are presented in Tables 4 and 5, respectively, to the first (yellow, red, blue, and purple plates) and second (white, black, gray and green plates) clustering analysis. In Table 4, a high frequency of geometric shapes I and II (Figure 6) are connected to the sprinkler operating with rotating plates (yellow and red). Although, geometric shapes III and IV (Table 4) appeared more often for the sprinkler attached to fixed deflector plates blue and purple.

Table 4. Representative water distribution curves for the sprinkler with deflector plates of yellow, red, blue, and purple as a function of nozzle diameter (4.5 and 5.6 mm), working pressure (103 and 138 kPa), and sprinkler height (0.8, 1.6, and 2.4 m).

Plate	Nozzle (mm)	103 kPa			138 kPa		
		0.8 m	1.6 m	2.4 m	0.8 m	1.6 m	2.4 m
Yellow	4.4	I	II	II	II	II	II
	5.6	I	II	II	I	II	IV
Red	4.4	I	II	I	II	II	I
	5.6	III	I	III	I	I	III
Blue	4.4	III	III	IV	III	III	IV
	5.6	III	III	III	III	I	IV
Purple	4.4	III	IV	IV	III	IV	IV
	5.6	III	IV	IV	III	III	IV

Regarding the sprinkler setup with white, black, gray, or green fixed deflector plates (Table 5), water distribution shapes I and II were observed more often for the white deflector plate, the geometric shape II for the green one, and patterns III and IV had a high frequency for black and gray plates. Ouazaa et al. (2014) pointed out that although fixed deflector plates produce a water distribution curve with a ring shape, the amount of water accumulated at the wetted circle edge depends on the combination of nozzle diameter and working pressure.

Table 5. Representative water distribution curves for the sprinkler with deflector plates of white, black, gray, and green as a function of nozzle diameter (4.5 and 5.6 mm), working pressure (103 and 138 kPa), and sprinkler height (0.8, 1.6, and 2.4 m).

Plate	Nozzle (mm)	103 kPa			138 kPa		
		0.8 m	1.6 m	2.4 m	0.8 m	1.6 m	2.4 m
White	4.4	I	I	II	I	II	II
	5.6	I	I	II	I	II	II
Black	4.4	III	III	I	IV	III	I
	5.6	IV	III	III	III	III	II
Gray	4.4	IV	IV	III	IV	III	III
	5.6	IV	IV	IV	IV	I	IV
Green	4.4	II	II	II	II	II	II
	5.6	II	II	II	II	II	II

Running laboratory tests for rotating and fixed sprinkler deflector plates and simulating the water distribution uniformity for sprinklers spaced in 1.5, 3.0, and 4.5 m on a lateral line of a center pivot irrigation system, Jiao et al. (2017) determined uniformity values from 85.8 to 91.7% and 85.8 to 86.2, respectively for the two plates evaluated. In field water distribution tests of a center pivot under different wind speeds, Lourenço (2018) measured water distribution uniformities from 85 to 97% and 79.9 to 94.2%, respectively, to rotating and fixed sprinkler deflector plates. Therefore, the sprinklers with rotating deflector plates provide higher uniformity values than the fixed plates.

CONCLUSIONS

Rotating deflector plates result in larger wetted radii than fixed plates.

Altering the sprinkler mounting height by one meter, there is a mean variation of 1.07 m on the wetted radius.

Four geometric shapes are sufficient to represent the water distribution curves of the sprinkler working with yellow, red, blue, or purple plates, as well as white, black, gray, or green plates.

Rotating plate sprinklers (yellow and red) should be preferred, as water distribution curves present a decrease in the application rate over the wetted radius.

REFERENCES

AL-GHOBARI, H.; DEWIDAR, A. Z. A comparative study of standard center pivot and growers-based modified center pivot for evaluation uniformity coefficient and water distribution. **Agronomy**, v.11, n.8, p.1-13, 2021. http://doi:10.3390/agronomy11081675

ANA – Agência Nacional de Águas e Saneamento Básico. **Atlas irrigação: uso da água na agricultura irrigada**. 2. ed. Brasília: ANA, 2021. 130 p.

BURDEN, R. L.; FAIRES, J. D. **Análise numérica**. São Paulo: Pioneira Thomson Learning, 2003. 740 p.

CHARFI, I. B.; CORBARI, C.; SKOKOVIC, D.; SOBRINHO, J.; MANCINI, M. Modeling of water distribution under center pivot irrigation technique. **Journal of Irrigation and Drainage Engineering**, v.147, n.7, p.1-10, 2021. http://doi:10.1061/(ASCE)IR.1943-4774.0001571

CHRISTIANSEN, J. E. **Irrigation by sprinkling**. Berkeley: California Agricultural Station, 1942. 124 p. Bulletin, 670

HUI, X.; ZHENG, Y.; YAN, H. Water distributions of low-pressure sprinklers as affected by the maize canopy under a centre pivot irrigation system. **Agricultural Water Management**, v.246, 106646, p.1-10, 2021. http://doi:10.1016/j.agwat.2020.106646

INTERNATIONAL ORGANIZATION FOR STANDARDIZATION. ISO 8026. **Agricultural irrigation equipment – Sprayers: General requirements and test methods**. Geneva, 2009. 18p.

JIAO, J.; WANG, Y.; HAN, L.; SU, D. Comparison of water distribution characteristics for two kinds of sprinkler used for center pivot irrigation systems. **Applied Science**, v.7, n.4, p.1-17, 2017. http://doi:10.3390/app7040421

LIU, J.; ZHU, X.; YUAN, S.; WNA, J.; CHIKANGAISE, P. Hydraulic performance assessment of sprinkler irrigation with rotating spray plate sprinkler in indoor experiments. **Journal of Irrigation and Drainage Engineering**, v.144, n.8, p.1-7, 2018.

http://doi:10.1061/(ASCE)IR.1943-4774.0001333

LOURENÇO, R. D. S. **Modelagem das perdas por evaporação e arraste em emissores de placa defletora fixa e rotativa oscilante na irrigação via pivô central.** 2018. 51 f. Dissertação (Mestrado em Engenharia Agrícola) – Universidade Federal de Viçosa, Viçosa.

OUAZAA, S.; BURGUETE, J.; PANIAGUA, M. P.; SALVADOR, R.; ZAPATA, N. Simulating water distribution patterns for fixed spray plate sprinkler using the ballistic theory. **Spanish Journal of Agricultural Research**, v.12, n.3, p.850-863, 2014. http://doi:10.5424/sjar/2014123-5507

PRADO, G. Water distribution from medium-size sprinkler in solid set sprinkler systems. **Revista Brasileira de Engenharia Agrícola e Ambiental**, v.20, n.3, p.195-201, 2016. http://doi:10.1590/1807-1929/agriambi.v20n3p195-201

PRADO, G.; COELHO, T. B. B.; TINOS, A. C.; MAHL, D.; BORTOLETTO, E. C. Distribuição de água de microaspersor para diferentes condições operacionais. **Irriga**, v.26, n.4, p.867-883, 2021. http://doi:10.15809/irriga.2021v26n4p867-883

ROVELO, C. O. R.; RUIZ, N. Z.; TOLOSA, J. B.; FÉLIX, J. R.; LATORRE, B. Characterization and simulation of a low-pressure rotator spray plate sprinkler used in center pivot irrigation systems. **Water**, v.11, n.8, p.1-20, 2019. http://doi:10.3390/w11081684

SAYYADI, H.; NAZEMI, A. H.; SADRADDINI, A. A.; DELIRHASANNIA, R. Characterising droplets and precipitation profiles of a fixed spray-plate sprinkler. **Biosystems Engineering**, v.119, p.13-24, 2014. http://doi:10.1016/j.biosystemseng.2013.12.011

SOLOMON, K.; BEZDEK, J. C. Characterizing sprinkler distribution patterns with a clustering algorithm. **Transactions of the American Society of Agricultural Engineers**, v. 23, n. 4, p. 899- 906, 1980. http://doi:10.13031/2013.34683

VALENCIA, A.; BRIGGS, J.; JACOB, S.; MARSHALL, A. Near field spray measurements for fixed spray plate sprinkler. **Irrigation Science**, v.37, n.1, p.597-609, 2019. http://doi:10.1007/s00271-019-00640-8

WANG, J.; SONG, Z.; CHEN, R.; YANG, T.; TIAN, Z. Experimental study on droplet characteristics of rotating sprinkler with circular nozzles and diffuser. **Agriculture**, v.12, n.7, p.1-21, 2022. http://doi:10.3390/agriculture12070987

ZHANG, Y.; GUO, J.; SUN, B.; FANG, H.; ZHU, D.; WANG, H. Modeling and dynamic-simulation the water distribution of a fixed spray-plate sprinkler on a lateral-move sprinkler irrigation system. **Water**, v.11, n.17, p.1-20, 2019. http://doi: 10.3390/w11112296